ISSN 1063-7834, Physics of the Solid State, 2008, Vol. 50, No. 6, pp. 1186–1190. © Pleiades Publishing, Ltd., 2008.
Original Russian Text © A.N. Titov, Yu.M. Yarmoshenko, A. Zimina, M.V. Yablonskikh, A.V. Postnikov, S. Eisebitt, 2008, published in Fizika Tverdogo Tela, 2008, Vol. 50, No. 6, pp. 1138–1142.

## LOW-DIMENSIONAL SYSTEMS AND SURFACE PHYSICS

# Absorption Spectroscopic Study of the Conduction Band of Titanium Dichalcogenides

**A. N. Titov[a], Yu. M. Yarmoshenko[a], A. Zimina[b], M. V. Yablonskikh[c], A. V. Postnikov[d], and S. Eisebitt[b]**

[a] *Institute of Metal Physics, Ural Division, Russian Academy of Sciences, ul. S. Kovalevskoĭ 18, Yekaterinburg, 620219 Russia*
*e-mail: yarmoshenko@ifmirs.uran.ru*
[b] *BESSY GmbH, Berlin, 12489 Germany*
[c] *Deptartment of Physics and Engineering Physics, University of Saskatchewan, Saskatoon, S7N 5E2 Canada*
[d] *Paul Verlaine University-Institute de Physique Electronique et Chimie, Laboratoire de Physique des Milieux Denses, Metz, F-57078 France*

Received October 22, 2007

**Abstract**—The $L_{2,3}$ spectra of titanium in the layered compound $TiSe_2$ and intercalated compounds $Fe_{1/2}TiSe_2$, $Cr_{1/3}TiSe_2$ and $Fe_{1/4}TiTe_2$ are studied. Theoretical calculations of the electronic structure of these compounds are performed. The experimental data and calculations suggest that the intercalation of the Cr and Fe atoms into the $TiSe_2$ matrix brings about a partial filling of the Ti 3*d* states and the spin polarization of the Cr 3*d* and Fe 3*d* states. Chemical bonds are formed through the hybridization of the *d* orbitals of intercalated atoms with the Ti 3*d*–Se 4*p* states of the matrix.

PACS numbers: 73.20.At, 79.60.-i

**DOI:** 10.1134/S1063783408060292

## 1. INTRODUCTION

Titanium dichalcogenides are presently widely used as electrode materials in electrochemical devices. The widest application they enjoy is as cathodes in lithium-based storage cells. The emf in the cell appears as a result of the Fermi level positions in lithium metal and the cathode material being different, and the current is generated by electron promotion from the metal to the titanium dichalcogenide conduction band, which derives primarily from the Ti 3*d* orbitals. It is the position and shape of the Ti 3*d* band that determine the magnitude of the emf, the cell capacity and, hence, the cell efficiency.

It has thus far been established [1] that the shape of the Ti 3*d* band is determined by the nearest chalcogen-atom environment of the titanium atom forming a distorted octahedron aligned with the hexagonal *c* axis. It is known that replacement of a chalcogen of one type with another, just as intercalation by transition and noble metals, gives rise to a change in the character of the chalcogen octahedron distortion [2]. This change should bring about a noticeable change in the shape and, possibly, of the energy position of the Ti 3*d* band.

On the other hand, intercalation by transition metals can result in redistribution of the electron density, mixing of Ti 3*d* states with the valence-band states of the intercalant and a change in the Ti 3*d* band filling. This effect may coexist with strains in the local environment of the chalcogen atoms. These two effects can be separated by comparing the materials in which strain is clearly pronounced for a negligibly small charge transport from the intercalant to the matrix titanium, on the one hand, with those featuring very small strain for a marked charge transport, on the other.

This statement can be directly verified in experiment by studying Ti x-ray absorption spectra. Regrettably, the available relevant experimental data are extremely scarce. There is only one experimental study on the $Fe_xTiSe_2$ system [3], which deals with investigation of Ti absorption spectra in this material as functions of the iron content. It should be pointed out that this system is the least structurally sensitive to variation of the intercalant content [4], which does not permit one to estimate the effect of intercalation on the position and shape of the Ti 3*d* band.

The dependence of the extent of lattice strain on intercalation is presented in [4]. The data reported suggest that insertion of Fe and Cr causes approximately the same strain. While, however, the divalent state of the intercalated iron is reliably established, it is $Cr^{3+}$ that is the stable state of chromium. For such materials one may expect different charge transport from the intercalated metal to the matrix for about the same lattice strain resulting from intercalation. This is why

these two materials are of particular interest for our study. A similar situation is observed with $Fe_{0.5}TiSe_2$ and $Fe_{0.25}TiTe@2$, where the charge state of Fe is the same whereas the strains are different [5, 6].

Studies of these materials are curtailed by the absorption spectra in the soft x-ray region being sensitive to the state of the surface. High-quality spectra can be obtained only from a clean surface of a crystal as-cleaved in high vacuum. Therefore, the spectra are studied only on single crystals of intercalated compounds that can be grown only for certain intercalant concentrations. This narrows the area within which one can investigate the effect of concentration on the conduction band structure of titanium dichalcogenides and of their intercalated compounds.

## 2. EXPERIMENT

The $TiL_{2,3}$ x-ray absorption spectra (XAS) were obtained by the total electron yield (TEY) and fluorescence yield (FY) methods on the BESSY synchrotron (Berlin, BESSY beamline UE-56/1-SGM, energy resolution 0.1 and 0.6 eV for the TEY and FY measurements, respectively) on the following materials: $TiSe_2$, $Fe_{0.5}TiSe_2$, $Cr_{0.33}TiSe_2$, and $Fe_{0.25}TiTe_2$. The measurements were performed on single crystals whose clean surface was obtained by cleaving directly in the spectrometer chamber in high vacuum.

The effect of local coordination of titanium on the shape and energy position of the conduction band should be investigated allowing, in addition to intercalation, for the actual type of the chalcogen coordinating the titanium atoms. In an ideal structural model, the width of the interlayer gap is assumed to be equal to that of the Se–Ti–Se layer itself. In this case, the relative Se coordinate $zc_0 = 0.25$, titanium has an ideally octahedral environment, and the lattice parameter ratio is $c_0/a_0 = 1.633$ [2]. According to the available structural data for titanium dichalcogenides and their intercalated compounds, however, the Se coordinates differ from 0.25 [2]. If this is so, then the width of the interlayer gap is no longer equal to the layer width, and the local Ti environment is characterized by the parameter $\gamma = 2zc_0/a_0$, which determines the width of the Se–Ti–Se layer and the titanium coordination in it. In an ideal octahedron, $\gamma = 0.8165$. Of the materials discussed in the present study, the corresponding structural data are known for $TiSe_2$ and $Fe_{0.5}TiSe_2$ only [7]. The latter material has monoclinic structure, which results in the selenium atoms being inequivalent, i.e., having different coordinates $z/c$. We believe that the strain should be estimated using an averaged quantity $zc$. Structural studies of the other materials were carried out by the full-profile analysis (see the table) at room temperature (DRON-1-UM, Ni filter, Cu$K_\alpha$ radiation, program package GSAS). The electronic structure was calculated by the FLAPW method with the WIEN2k code [8].

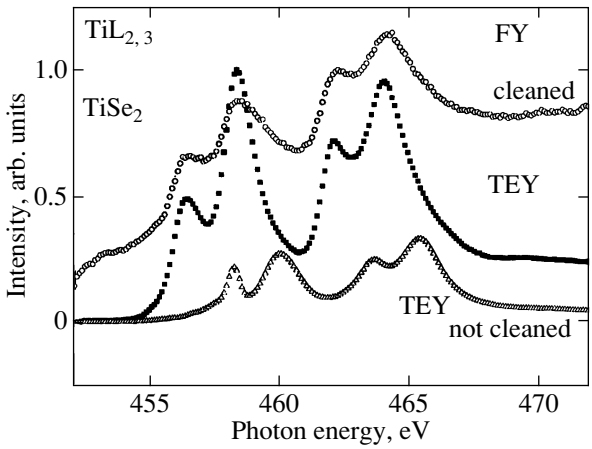


**Fig. 1.** Ti $L$ absorption spectra of the $TiSe_2$ compound.

## 3. RESULTS AND DISCUSSION

We start with a qualitative comparison of the spectra and calculations of the compounds under study using the structural parameters obtained in the present work. All these compounds belong to the $CdI_2$ structural type (rhombohedral symmetry, space group $P\bar{3}m1$).

The table lists the corresponding lattice parameters. Also given are the distortions of the cell (consisting of two $TiX_6$ octahedra) $2c_0z/a_0$. Figure 1 presents Ti $L_3$ spectra of the as-cleaved $TiSe_2$ crystal surface (identified as "cleaned") and of the as-grown surface (labeled "not cleaned"). The spectra of the cleaved and as-grown surfaces differ in the energy position and relative spectral band intensity. The spectrum of the as-grown surface is practically identical in its energy position and shape with that of $TiO_2$ [9], which supports the need for using a cleaved surface.

The Ti $L_3$ spectrum of $TiSe_2$ exhibits two clearly pronounced bands peaking at 456.3 and 459.3 eV (Fig. 1). The TEY and FY spectra are identical in the information they offer and differ only in instrumental resolution. They are presenter together in Fig. 1 to support our use of the TEY method as requiring a comparatively short time for obtaining good quality spectra.

Structural parameters of intercalated titanium dichalcogenides according to the x-ray profile analysis of powder samples at room temperature

| Compound | $a$, Å | $b$, Å | $c$, Å | $2zc/a$ |
|---|---|---|---|---|
| $TiSe_2$ | 3.540 | 3.540 | 6.008 | 0.8655 |
| $TiTe_2$ | 3.766 | 3.540 | 6.008 | 0.9042 |
| $Cr_{1/3}TiSe_2$ | 3.589 | 3.589 | 6.491 | 0.8651 |
| $Fe_{1/2}TiSe_2$ | 6.2673 | 3.5915 | 11.9557 | 0.8552 |
| $Fe_{1/4}TiTe_2$ | 3.8109 | 3.8109 | 6.3451 | 0.8842 |

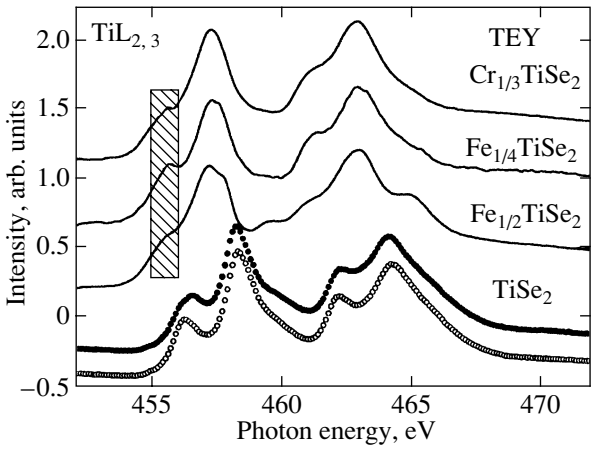


**Fig. 2.** Ti L absorption spectra of the $TiSe_2$ and $TiTe_2$ compounds intercalated by Cr and Fe. Shown below are the spectra of pure $TiSe_2$ measured in different geometries under normal (closed circles) and grazing (open circles) x-ray beam incidence.

We consider now the Ti $L$ XAS spectra of cleaved and chromium-intercalated titanium diselenide (Fig. 2). The two bands observed in the Ti $L_3$ (as well as Ti $L_2$) spectrum are assigned to $e_g$ and $t_{2g}$ orbitals into which the $d$ wave functions of a metallic atom split in octahedral environment. The energy splittings between the $e_g$ and $t_{2g}$ bands of the two compounds under consideration differ by 0.3 eV, namely, 1.9 eV for $TiSe_2$ and 1.6 eV for $Cr_{1/3}TiSe_2$, respectively. The $t_{2g}$ band in the intercalated compound is weaker. These experimental data match qualitatively with the model calculations [10] which suggest that as the distortion decreases, the $e_g$ and $t_{2g}$ orbitals degenerate to merge into one band.

Although the $\gamma$ parameter of $Cr_{1/3}TiSe_2$ only marginally differs from that of $TiSe_2$ (see table), the spectrum changes noticeably as a whole both in the relative intensity of the bands and in their energy position. We note a comparatively large increase of the lattice parameter $c_0$ in $Cr_{1/3}TiSe_2$ against that in $TiSe_2$.

We can compare the effect of octahedral distortion on formation of the electronic structure of the three intercalated compounds on a common scale of the crystal phase type considered here (Fig. 2). The energy splitting between the two lower lying bands in the spectra is nearly the same for the compounds under study. They lie energywise at 555.6 and 557.2 eV. As seen from Fig. 2, the contrast between the two split bands in this energy region is maximal for the spectrum of $Fe_{1/4}TiTe_2$. This behavior correlates well with the octahedral distortion in this compound being the largest compared with the others (see table).

The distortion of the crystal structure, which is discussed when analyzing the spectra and, in the final count, the electronic structure of both compounds, is not the major factor responsible for the variation of the spectrum. In $Cr_{1/3}TiSe_2$, the valence band is additionally populated by Cr 3$d$ electrons, which gives rise to spatial polarization of Se atoms in the formation of Cr–Se–Ti bonds and, according to our measurements, to an increase of the binding energy of the inner Ti2$p_{3/2}$ level by 0.5 eV from the original value of 455.0 eV.

In $Cr_{1/3}TiSe_2$, chromium is oxidized to the 3+ state, and, therefore, the lowest empty Ti3$d_{z^2}$-like bands are populated in the intercalated state by one electron per formula unit. In the other compounds ($Fe_{1/4}TiTe_2$ and $Fe_{1/2}TiSe_2$) these bands contain 0.5 and 1 electron, accordingly. This difference in population becomes reflected in the shape of the titanium spectrum in these two compounds as well. An increase in population of the Ti 3$d$ band in $Fe_{1/2}TiSe_2$ compared with $Fe_{1/4}TiTe_2$ becomes manifest in the titanium absorption spectrum in a decrease of relative intensity and smoothing of the spectral subband in the hatched energy region of 455–456 eV (Fig. 2).

Figure 3 plots the density-of-states functions for $TiSe_2$, $Cr_{1/3}TiSe_2$, and $Fe_{1/4}TiTe_2$. We note immediately that the metallic 3$d$ states of any orbital symmetry are seen to exist throughout the valence band region in these compounds. This conclusion is experimentally corroborated. Shown at the bottom of Fig. 2 are two matched Ti$L_{2,3}$ spectra of $TiSe_2$ obtained under normal and grazing incidence of the x-ray beam on the $TiSe_2$ single crystal surface. These spectra provide an idea of the distribution in energy of Ti 3$d$ states having different spatial symmetries. Unlike the absorption spectrum measured under grazing angle of incidence, the one obtained under normal incidence has no contribution of the Ti Ti3$d_{z^2}$ orbital altogether. The spectra measured under both crystal orientations are nearly identical. This argues for the titanium orbitals being energywise delocalized. The calculations permit one to separate the Cr 3$d$ and Fe 3$d$ contributions in symmetry on the energy scale only in special cases where the number of states of a given symmetry is dominant in some energy interval. For instance, in the unoccupied part of the valence band $3d_{xz, yz}$ states are dominant at energies above +2 eV. Nevertheless, the overall patterns of the distribution in energy of Cr 3$d$ and Fe 3$d$ states in the diselenide and ditelluride, accordingly, differ substantially. Calculations show convincingly that Cr 3$d$ states reveal typically a trend to localization as compared with the Fe 3$d$ states. The centers of gravity of chromium 3$d$ states with different spin projections are located energywise fairly far on both sides of the Fermi level, while near –0.7 eV one observes a gap for spin-up occupied states. A similar gap $\Delta E = 0.5$ eV in the region of unoccupied states lies near +2 eV. The region of Cr Cr3$d_{z^2}$ states in Fig. 3 is blackened with the purpose to permit determination of contributions of states with different orbital symmetries to hybridization with selenium and

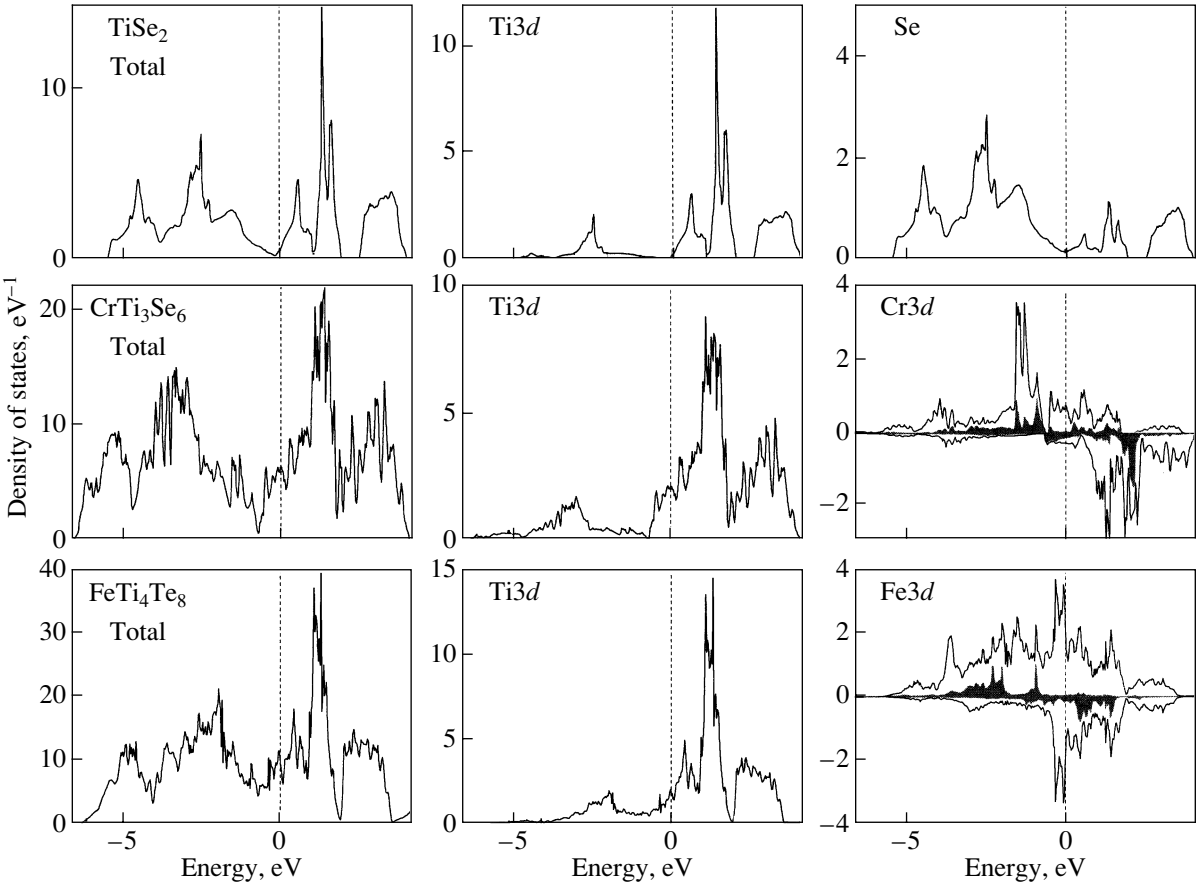


**Fig. 3.** Calculated density-of-states function for the $TiSe_2$, $Cr_{1/3}TiSe_2$, and $Fe_{1/4}TiTe_2$ compounds. The Cr $3d_{z^2}$ and Fe $3d_{z^2}$ states are hatched.

titanium. The Cr3$d_{z^2}$ states are spread out within a broad energy interval, and the maximum of their distribution in the unoccupied part of the valence band lies at +2 eV. In the vicinity of this energy, the Ti 3*d* spin-up states have a gap, and the density of states with the opposite spin projection is low. The lower-lying unoccupied 3*d* states of chromium with another orbital symmetry occupy the same energy interval with the Ti 3*d* states. The Se environment mediates their mixing. In the occupied part of the valence band a similar situation prevails. At energies from –1 to –2 eV, where the density of Cr 3*d* (including $d_{z^2}$) states reaches a maximum, the density of Ti 3*d* states is minimal. An analysis of the distribution of Se states in the valence band suggests that all the 3*d* states of chromium, with the exception of $d_{z^2}$, mix with Se states. One may therefore conclude that incorporation of chromium favoring valence band filling brings about hybridization of primarily unoccupied 3*d* states of titanium and chromium. This chemical bond forms as a result of charge polarization at selenium layers bordering both ($TiSe_6$ and $CrSe_6$) octahedra. Polarization is initiated by mixing of the Se4*sp* and Cr 3*d* orbitals. The Cr 3*d* orbitals is practically not involved in this process. The strong localization of the Cr 3*d* states is suggested by studies of x-ray photoelectron spectra [11], where one observed a 1-eV exchange magnetic splitting of the Cr $2p_{3/2}$ spectrum.

As already mentioned, in contrast to $Cr_{1/3}TiSe_2$, in the valence band of $Fe_{1/4}TiTe_2$ there is 0.5 electron per formula unit. This brings about noticeable differences in the Fe 3*d* density of states distribution (Fig. 3). Near the Fermi level, one observes a narrow Fe 3*d* spin-polarized band of high intensity. This band is weakly hybridized with Ti 3*d* states in this energy region. At energies about 1.7 eV above the Fermi level, one can observe a Fe$d_{z^2}$ band mixed with a strong Ti 3*d* band. As in $Cr_{1/3}TiSe_2$, the 3*d* states of Fe and Ti interact because of their being hybridized with valence states of bordering tellurium atoms. Note that the lattice parameter $\mathbf{c}_0$ in $Fe_{1/4}TiTe_2$ is smaller than that in $Cr_{1/3}TiSe_2$ (see table). This provides favorable conditions for direct interaction between the $d_{z^2}$ orbitals of iron and titanium atoms.

## 4. CONCLUSIONS

The analysis of the experimental spectra and the results of the calculations of the densities of states has demonstrated that the formation of the electronic structure of the dichalcogenides considered in this study is affected by two competing mechanisms. One of them consists in filling the lowest empty Ti 3*d*-like band and is determined by the valence and the concentration of intercalated atoms. The other mechanism is based on the effect of octahedral distortions of different extents on the hybridization of the 3*d* states of the impurity with the Ti 3*d* and *X p* states (*X* = Se, Ti).

## ACKNOWLEDGMENTS

This study was supported by the Russian Foundation for Basic Research, project no. 06-03-32900.

## REFERENCES

1. R. H. Friend and A. D. Yoffe, Adv. Phys. **36**, 1 (1987).
2. T. Hibma, *Intercalation Chemistry*, Ed. by M. S. Wittingham and A. J. Jacobsen (Academic, London, 1982), p. 285.
3. A. Yamasaki, S. Imada, H. Itsunomiya, T. Muro, Y. Saitoh, H. Negishi, M. Sasaki, and S. Suga, Physica E (Amsterdam) **10**, 387 (2001).
4. Y. Arnaud, M. Chevreton, A. Ahouanjiou, M. Danot, and J. Rouxel, J. Solid State Chem. **17**, 9 (1976).
5. D. R. Huntley, M. I. Sienko, and K. Hiebel, J. Solid State Chem. **52**, 233 (1974).
6. V. G. Pleshchev, A. N. Titov, S. G. Titova, and A. V. Kuanov, Neorg. Mater. **33** (11), 1333 (1997) [Inorg. Mater. **33** (11), 1128 (1997)].
7. G. Calvarin, J. R. Gavarri, M. A. Buhannic, P. Colombet, and M. Danot, Rev. Phys. Appl. **22**, 1131 (1987).
8. P. Blaha, K. Schwarz, G. K. H. Madsen, D. Kvasnicka, and J. Luitz, *WIEN2k: An Augmented Plane Wave Plus Local Orbitals Program for Calculating Crystal Properties* (Karlheinz Schwarz Technological Universität, Vienna, Austria, 2001).
9. F. M. F. de Groot, J. Electron Spectrosc. Relat. Phenom. **62**, 111 (1993).
10. R. Huisman, R. de Jonge, C. Haas, and F. Jellinek, J. Solid State Chem. **3**, 56 (1977).
11. A. V. Postnikov, M. Neumann, St. Plogmann, Yu. M. Yarmoshenko, A. N. Titov, and A. V. Kuranov, Comput. Mater. Sci. **17**, 450 (2000).

*Translated by G. Skrebtsov*

SPELL: OK